J. Pharm. Pharmacol. 1997, 49: 377–383
Received October 16, 1996
Accepted November 28, 1996

Modelling of the Void Space of Tablets Compacted Over a Range of Pressures

CATHY J. RIDGWAY, KENNETH RIDGWAY* AND G. PETER MATTHEWS

*Department of Environmental Sciences, University of Plymouth, Drake Circus, Plymouth, Devon and *Reading, Berkshire, UK*

Abstract

A previously developed computer model, named Pore-Cor, has been used to simulate the changes in the void-space dimensions which occur during the compaction of tablets over a range of pressures.

The tablets were made by mixing pharmaceutical grade crystalline lactose and an anti-inflammatory compound in the proportion 4:1. Compacts were made by placing a weighed amount of the mixed powder into a stainless-steel die and applying pressure with a hand-operated calibrated hydraulic press. Compacts were prepared at eight pressures over the hydraulic pressure range 1 to 8 ton in^{-2} (15·4–123·2 MPa) in 1 ton in^{-2} increments. Mercury-intrusion curves were measured for the eight samples by use of a porosimeter and the Pore-Cor package was then used to simulate the mercury-intrusion curves and generate void-space models of the correct porosity.

The experimental and simulated characteristic throat diameter, the experimental and simulated porosity, and the simulated permeability of the tablets have all been shown to follow expected trends. The successful modelling of void-structure parameters, which are difficult or impossible to measure experimentally, opens the way to an improved understanding of the strength of compacts.

As the compaction pressure applied to a tablet is increased, the density of the compact increases and its porosity decreases. This effect has been demonstrated in computer simulations by Lu & Shi (1994). The strength of compacts is dependent on their formulation, moisture content, and porosity (Leitritz et al 1996). The relationship between strength and void structure has been studied by Lustig et al (1996) in terms of surface-specific tensile strength but, as these authors point out, a more detailed knowledge of the void structure is required for full understanding of the relationship.

Mercury porosimetry is a method of measuring the size distribution of the void spaces in a compacted material: pressurized mercury is applied to the tablet, and the volume of mercury intruded into it is measured as a function of the applied pressure. The greater the applied pressure, the smaller the voids into which the mercury will be forced, so that a plot of the volume of mercury intruded against the applied pressure can also be plotted against the pore diameter. Most compacted materials yield a sigmoid curve from which parameters such as the mean pore-size can be determined. However, much more information about the detailed structure of the pores can be obtained by computer modelling. Pore-Cor, the principal topic of this paper, is a computer model that operates by considering an array of pores of various sizes arranged on a cubic lattice and connected by throats, also of various sizes. The model is of a representative unit-cell consisting of 1000 lattice sites. Initial constraints can be fed in by the operator, after which the computer will follow a successive approximation routine to fit a pore-size range and a throat-size range on to the lattice, and converge to an array that, were it to be subjected to mercury porosimetry, would give a curve closely following the actual experimental curve obtained for the real material. From the simulation, it is possible to arrive at values for parameters such as the throat- and pore-size distributions, the connectedness of the pores, the porosity and the permeability.

Correspondence: G. P. Matthews, Department of Environmental Sciences, University of Plymouth, Plymouth, Devon PL4 8AA, UK.

A brief review of void-space modelling

The Pore-Cor model itself has been used in a wide range of contexts, such as sandstones and other oil-bearing rocks, china clay, paper coatings, battery separators, tantalum slugs and building materials (Matthews & Spearing 1992; Matthews et al 1995a, b). It is based upon a percolation algorithm which incorporates the Washburn–Laplace equation. This equation relates the diameter of a void, the curvature of a mercury surface, and the mercury–solid–vacuum interfacial tension, to the applied mercury pressure at which the mercury will penetrate the void. The equation itself has many limitations which have been reviewed by Van Brakel et al (1981).

Further problems which arise from applying the Washburn-Laplace based percolation algorithm to a real porous substance (Garboczi 1991) are that the throats are all considered to be cylindrical, and that the mapping of the effective network derived from the mercury porosimetry curve is not necessarily the same as that of the real network. Mason et al (1988) investigated specific shapes of pores and also modelled the intrusion and extrusion of mercury in an array of packed spheres by using the Haines in-sphere approximation to model the void spaces between them (Haines 1927; Mason & Mellor 1991). By use of a range of rod- and plate-like structures Conner et al (1988) have shown that there is a relationship between the shapes of the pores and the throats, and the shapes of the mercury intrusion and extrusion hysteresis curves. Garboczi (1991), however, showed that a range of pores and throats of different shapes and sizes could be adequately represented by a random network of interconnecting elliptical cylinders ranging from circular (major and minor axes equal) through to cracks (minor axis negligible). As will be demon-

strated, the mercury-intrusion curve can be simulated quite satisfactorily using only a (circular) throat diameter distribution, a pore size to neighbouring throat diameter correlation, and connectivity.

Description of the Pore-Cor model

The Pore-Cor model has three main characteristics: a physically realizable geometry (Fig. 1); all fitting parameters are real experimentally-verifiable properties related to the geometry of the unit-cell; and the same network with precisely the same geometry can be used to model a wide range of properties. Properties already modelled are shown as solid boxes in Fig. 2, whereas properties to be developed, associated with enhanced oil recovery (EOR) and the opacity of paper coatings, are shown with dashed boxes.

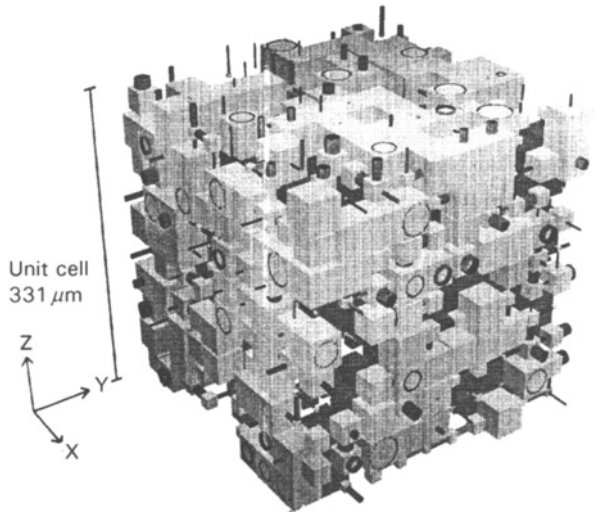

FIG. 1. Two outermost layers of the unit-cell for the 1-ton-in^{-2} tablet.

The void space within a porous solid can be regarded as a network of void volumes (pores) connected by a network of smaller void channels (throats). The Pore-Cor network comprises a three-dimensional cubic unit-cell which repeats infinitely in each direction, each cell containing 1000 nodes on a regular 10 × 10 × 10 matrix. Fig. 1 shows the two outermost layers of pores and throats in a unit-cell representing the void space of the 1-ton-in^{-2} tablet. It is apparent that the nodes are positioned using Cartesian co-ordinates x, y and z, although, because the sample is isotropic, the allocation of these axes is arbitrary. The origin of the axes is at the corner of the unit-cell adjacent to the first node. The void volume in the unit-cell comprises up to 1000 cubic pores centred on the nodes. Connected to each pore are up to six cylindrical throats along the axial directions in the positive and negative x, y and z directions. The number of throats connected to a particular pore is the 'pore co-ordination' number, and the arithmetic mean of this quantity over the whole unit-cell is the 'connectivity'. Individual pore co-ordination numbers can range from 0 to 6; the connectivity of sandstone is approximately 3 (Koplik et al 1984; Yanuka et al 1986).

The void-space model assumes that the throat diameter distribution is log-linear, i.e. the diameters are equally spaced

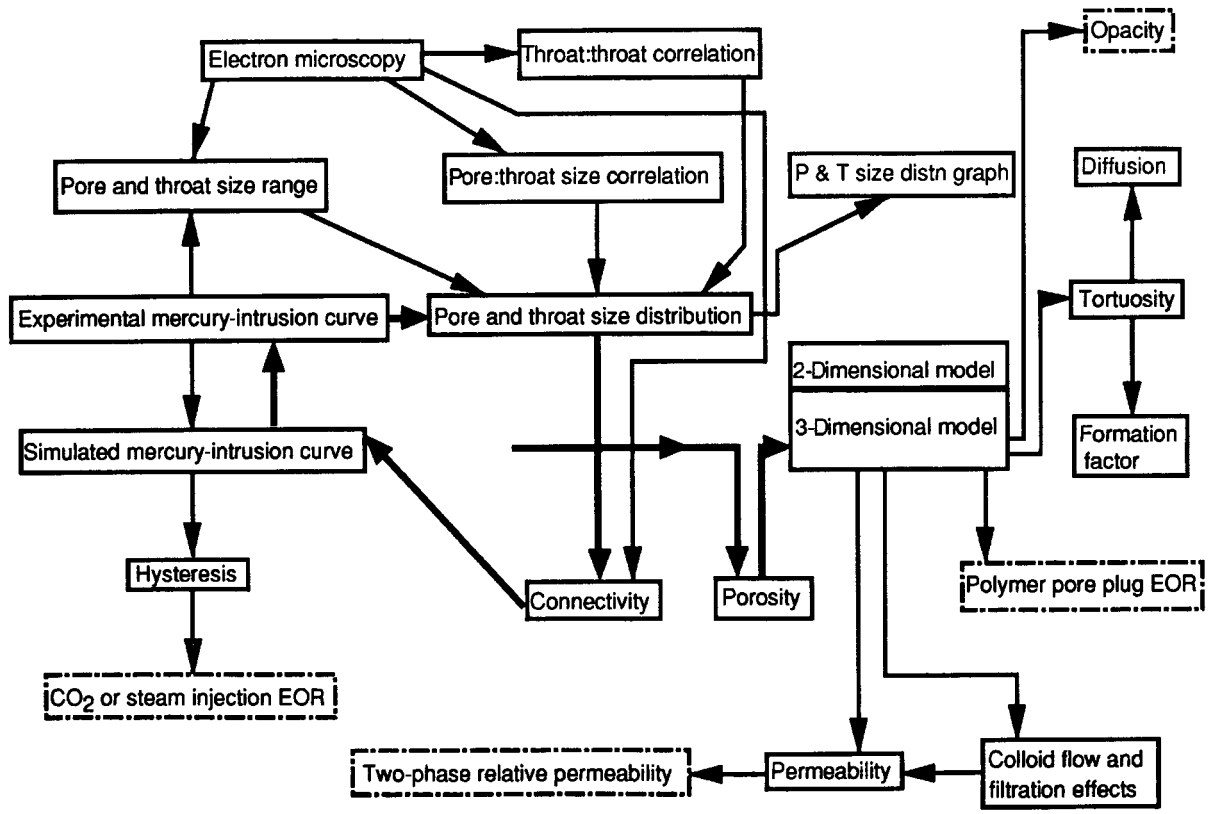

FIG. 2. Scope and data flow of Pore-Cor. Solid boxes show work to date, dashed boxes show future work, bold arrows show route of manual and automatic calculation methods.

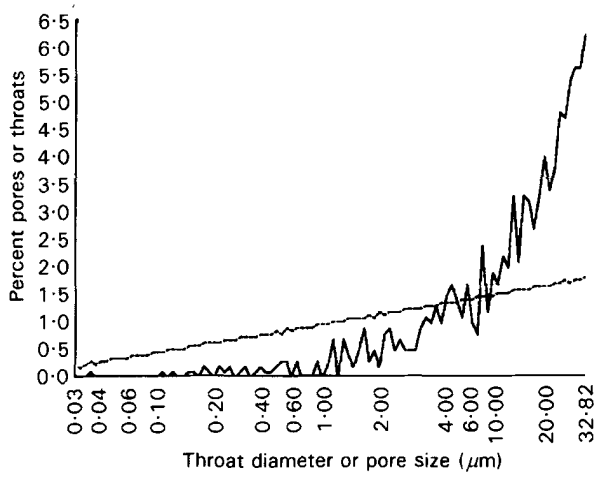

FIG. 3. Skewed (0.2%) throat-diameter distribution (- - -) and pore-size distribution (——).

over a logarithmic axis, as shown in Fig. 3. A log-normal distribution can also be used, but usually gives mercury-intrusion curves which are too steep at the point of inflection (the characteristic throat diameter). The parameters that can be varied are the range of throat diameters, the connectivity, the skew of the throat-diameter distribution, the skew of the pore-diameter distribution, the relationship between adjacent throat and pore sizes, and the spacing between the rows of pores. The gradient of the mercury-intrusion curve at its point of inflection is governed by the connectivity (Matthews et al 1995b). The term 'throat-skew' is the percentage of throats of the smallest size in a log-linear distribution. A throat-size distribution with a throat-skew of 0·2%, for example, has 0·2% of the smallest throat size, 1% of the size in the middle of the logarithmic distribution, and 1·8% of the largest size (Fig. 3). It is also possible for the throat-skew to be negative (Matthews et al 1996). The pore-skew parameter is a new parameter which has been introduced into Pore-Cor for the modelling of higher porosity samples. The whole pore-size distribution is multiplied by this number and then any pore whose size is larger than the original maximum of the range is truncated to this maximum pore size. This results in a frequency peak at the maximum of the pore size distribution, but enables larger porosities to be simulated. In the absence of specific experimental information, the size of each pore has been set equal to the diameter of the largest throat entering it, a correlation typical of sandstones but not limestones (Wardlaw et al 1987). The row spacing of the matrix is adjusted so that the porosity of the simulated network is equal to that of the experimental sample.

In the present mercury-intrusion simulation, the mercury is injected normal to the xy plane at $z = l_{cell}$, the unit-cell size, in the $-z$ direction. The injection corresponds to intrusion downwards from the top surface of Fig. 1. The unit-cell repeats infinitely in each direction, and therefore the simulation corresponds to intrusion into an infinite sheet of thickness l_{cell}.

Modelling the mercury-intrusion curve

In the Pore-Cor software package, the simulated mercury-intrusion curve can be made to converge automatically on to the experimental curve. Four criteria for closeness of fit have been described in previous publications: that the curves should cross at 50% pore volume (50% fit); that the mean-square deviation of simulated from experimental throat diameters should be a minimum (linear fit); that the mean-square deviation of the logarithms of simulated from experimental throat diameters should be a minimum (logarithmic fit); and that the mean-square deviation of simulated from experimental throat diameters should be a minimum for comparison points above the median point in the experimental curve (linear top fit). The deviations in the last three of these criteria are measured at experimental and interpolated points.

Materials and Methods

The material used to make the tablets was a mixture of pharmaceutical grade crystalline lactose, mean particle size 60 μm, with an anti-inflammatory compound that had a much smaller particle diameter, 2–6 μm; these were mixed in the proportion 80% lactose to 20% active ingredient. Mixing was achieved by brushing the roughly mingled powders through a 150-μm stainless-steel sieve, hand mixing, and brushing through the sieve again.

Compacts were made by weighing the mixed powder (0·8 g) into a 13-mm-diameter stainless-steel die and applying pressure. The powder was confined between two small discs, one above and one below the compact, which had mirror-finish faces to ensure an accurately plane-faced compact. Pressure was applied to the upper punch of the die assembly by means of a hand-operated calibrated hydraulic press (Perkin-Elmer), the peak applied pressure being maintained for 10 s. Compacts were prepared at eight pressures over the range 1 to 8 tons in^{-2} (15·4–123·2 MPa).

Mercury intrusion was performed for the eight samples using a Micromeritics AutoPore III porosimeter. The data were then corrected using the spreadsheet-based program Pore-Comp (Gane et al 1996) which uses a blank run correction with the Tait equation to correct for mercury compressibility and penetrometer expansion effects. The spreadsheet can also be used to correct for any compression of the solid phase of the sample. These final corrected data were then used with the Pore-Cor model, which simulated three-dimensional void-space structures. The simulated mercury-intrusion curves agreed with the experimental curves.

Results and Discussion

Intrusion curves were obtained for the eight tablet samples, after correction for mercury compressibility, penetrometer expansion and solid-phase compression. All the samples showed a compressibility of the solid phase (not the tablet as a whole) in the range 0·53–0·68 × 10^{-10} Pa. The corresponding bulk moduli are in the range 19–15 GPa showing the same level of compressibility as ground marble-latex mixtures used for paper coatings (Gane et al 1996). Fig. 4 shows the data for the 1-ton-in^{-2} tablet. The raw data are shown as squares, the data corrected for mercury compression and penetrometer expansion as diamonds, and the fully corrected data, where corrections have been made to take into account the com-

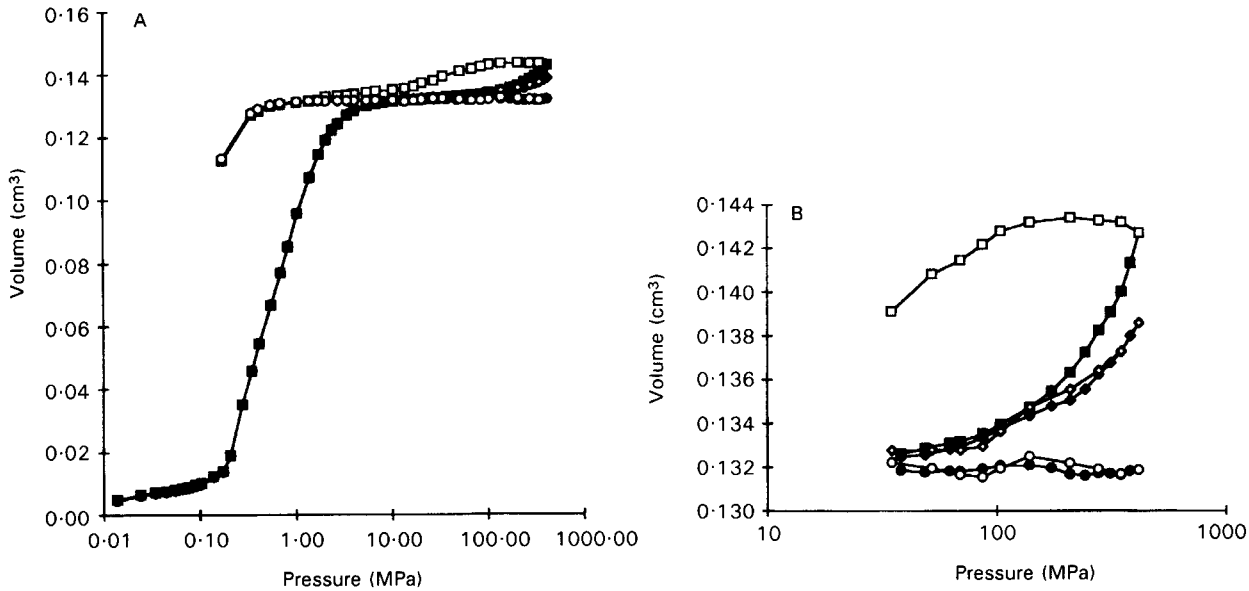

FIG. 4. A Corrected mercury-intrusion curves for 1-ton-in^{-2} tablet. ■ Raw intrusion data, ◆ intrusion data corrected for mercury and penetrometer effects, ● fully corrected intrusion data, □ raw extrusion data, ◇ extrusion data corrected for mercury and penetrometer effects, ○ fully corrected extrusion data. B Enlargement of top section of Fig. 4A.

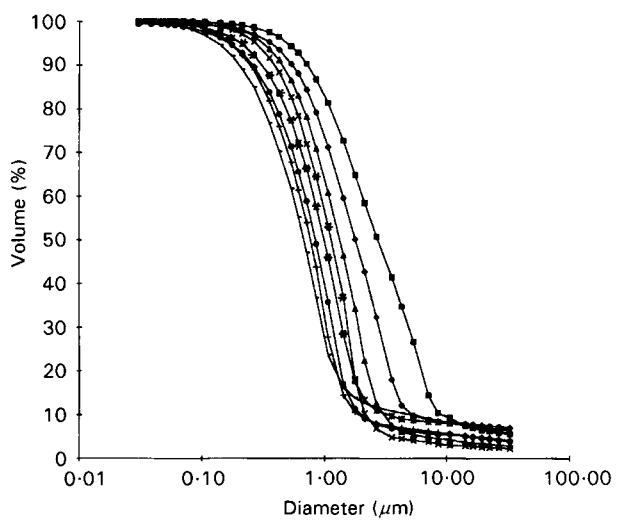

FIG. 5. Mercury-intrusion curves used with Pore-Cor. ■ 1 ton in^{-2}, ◆ 2 ton in^{-2}, ▲ 3 ton in^{-2}, × 4 ton in^{-2}, * 5 ton in^{-2}, ● 6 ton in^{-2}, + 7 ton in^{-2}, – 8 ton in^{-2}.

pressibility of the solid phase of the tablets, as circles. The solid shapes are the intrusion data and the outlined shapes are the extrusion data. Most of the intrusion points and many of the extrusion points are coincident. An enlargement of the top section of the graph, where the points diverge, is shown to the right of the figure (Fig. 4B). Similar graphs were obtained for the other seven samples. Fig. 5 shows the corrected intrusion data for the eight tablets compacted to pressures in the range 1–8 ton in^{-2}. The curve to the far right of the diagram is that for the tablet pressed to 1 ton in^{-2} as the pressure is increased the curves move to the left. Thus the experimental characteristic throat diameter is reducing as the tablet compression pressure is increased.

Modelling of pressed tablet samples

The logarithmic fitting criterion, as described earlier, was used as a measure of goodness of fit during convergence of Pore-Corsimulated intrusion curves on to the experimental curves shown in Fig. 5. The Pore-Cor throat-size range used for these samples was 0·030–32·82 μm, the parameters resulting from the optimum fitting of the simulated mercury-intrusion curve to the experimental mercury-intrusion curve being shown in Table 1. Fig. 6 shows the pore- and throat-size distributions resulting from the fitting of the simulated to experimental mercury-intrusion curve for the 4-ton-in^{-2} tablet. The simulated and experimental curves for this tablet are shown in Fig. 7.

Pore-Cor parameters

When these curves have been optimized to a best fit, it is possible to study the resulting fitting parameters in Table 1. Fig. 8 shows the trends of the connectivity, pore-skew and throat-skew. Fig. 5 showed all the intrusion curves and it can be seen that the slopes of these curves are very similar. There is a close connection between the connectivity and the slope of the curves (Matthews et al 1995b), hence the connectivities of these samples do not vary very much. Pore-skew is a parameter related to the porosity of the unit-cells, samples with high porosity having a higher pore-skew. As the porosity of this series of samples decreases, so, in general, does the pore-skew. The general trend of the throat-skew is to increase with increasing applied pressure on the compacts. This indicates that there are more of the smaller voids and fewer of the larger voids with increasing pressure and compaction, as would be expected.

The simulated and experimental characteristic throat diameters show a similar trend of reducing in size as greater pressure is applied to the compacts. These values are illustrated in Fig. 9, which also confirms the close fit of the simulation to

Table 1. The Pore-Cor parameters resulting from the optimum fitting of the simulated mercury-intrusion curves to the experimental mercury-intrusion curves.

	Compaction pressure of tablet (ton in^{-2}):							
	1	2	3	4	5	6	7	8
Pore-Cor simulated porosity (%)	42·31	37·42	28·33	25·01	23·76	21·39	19·41	17·75
Experimental characteristic throat diameter (μm)	2·726	1·783	1·326	1·131	0·989	0·839	0·764	0·673
Simulated throat characteristic diameter (μm)	3·006	2·123	1·487	1·116	1·131	0·851	0·795	0·498
Minimum pore and throat diameter (μm)	0·03	0·03	0·03	0·03	0·03	0·03	0·03	0·03
Maximum pore and throat diameter (μm)	32·82	32·82	32·82	32·82	32·82	32·82	32·82	32·82
Throat-skew	0·26	0·49	1·20	1·29	0·86	1·03	1·06	1·01
Connectivity	2·8	2·8	3·8	3·4	2·8	2·8	2·8	2·7
Pore-skew	1·6	1·6	1·8	1·5	1·3	1·3	1·4	1·2
Simulated permeability (mD)	0·423	0·109	0·0155	0·00241	0·00318	0·00127	0·00101	0·000518
Pore row spacing (μm)	33·16	33·47	35·30	33·02	33·83	33·60	35·70	34·57
Compressibility ($\times 10^{-10}$ Pa)	0·53	0·60	0·56	0·68	0·61	0·63	0·56	0·60
Bulk modulus (GPa)	18·9	16·8	18·0	14·7	16·4	15·8	18·0	16·8

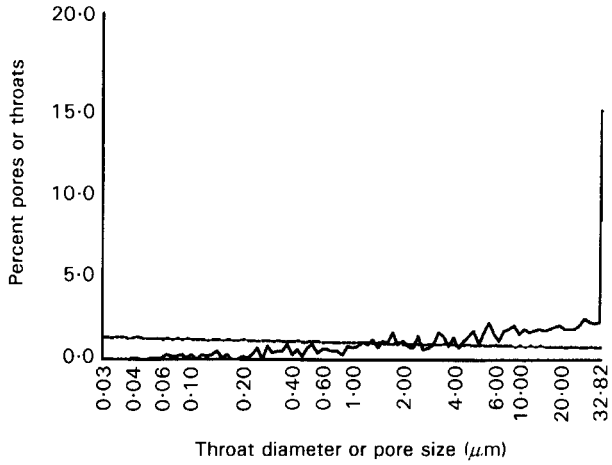

FIG. 6. Throat diameter —, and pore size - - -, distribution for 4-ton-in^{-2} tablet.

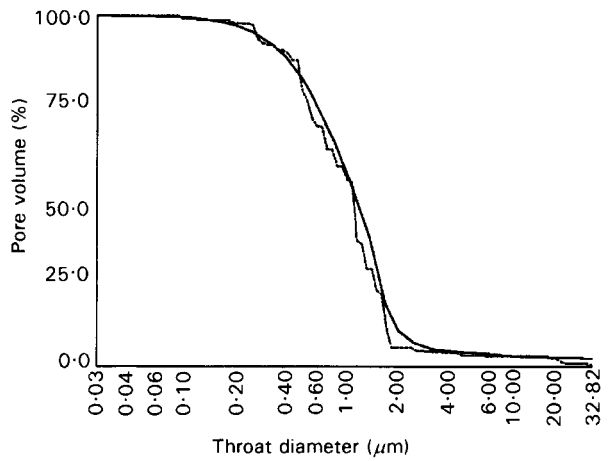

FIG. 7. Experimental —, and simulated - - -, mercury-intrusion curves for 4-ton-in^{-2} tablet.

the experimental data at the points of inflection. Fig. 10 shows the simulated permeabilities, expressed in milliDarcies (mD, where 1 Darcy = 9·87 $\times 10^{-13}$ m^2) for the eight samples on a logarithmic scale. Experience with other substances has

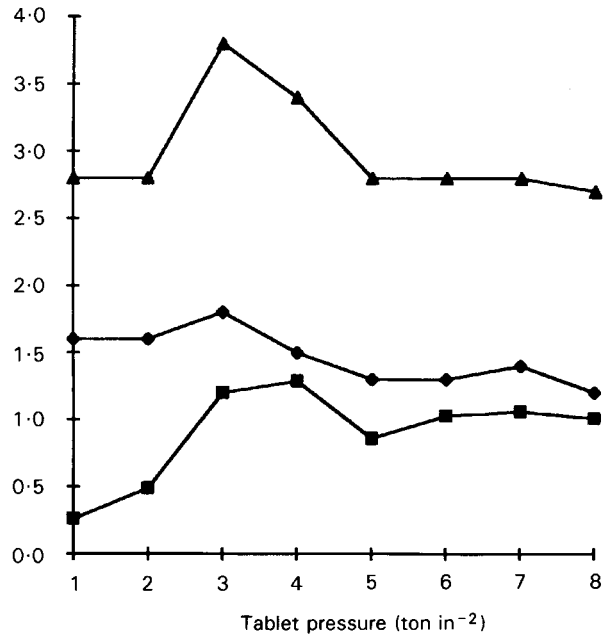

FIG. 8. Connectivity ▲, throat-skew ■, and pore-skew ●, values of compacted tablets.

demonstrated that the simulated permeabilities are usually substantially lower than experimental values, but that the trends in simulated permeability are correct. It is very evident in Fig. 10 that the simulated permeability is substantially reducing as the tablets are pressed to the higher pressure of 8 ton in^{-2}. Fig. 11 shows a similar trend with the porosities.

All these experimental results are as would be expected. The actual permeability could not be measured, because no permeameter is available for non-rigid samples. Pore-Cor has, however, simulated and illustrated the differences between these eight tablet samples compacted to a range of pressures.

The three-dimensional unit-cells for the 1-ton-in^{-2} and 8-ton-in^{-2} tablets are shown in Figs 1 and 12, respectively, only the two outermost layers being shown. The reduction in voidage in the 8-ton-in^{-2} tablet, compared with the 1-ton-in^{-2} tablet, can be clearly seen, giving a direct visual representation of the effect of increased compaction. In Pore-Cor modelling terms, the pore-skew parameter, which corresponds to the

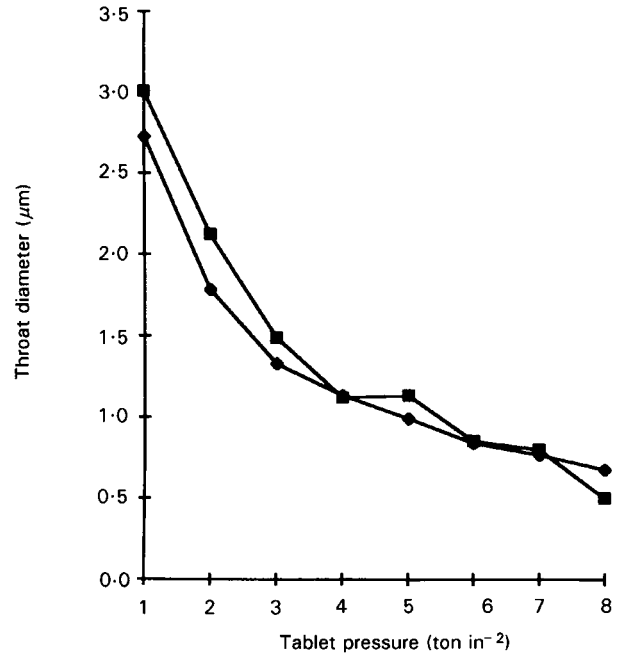

FIG. 9. Experimental ◆, and simulated ■, characteristic throat diameters of compacted tablets.

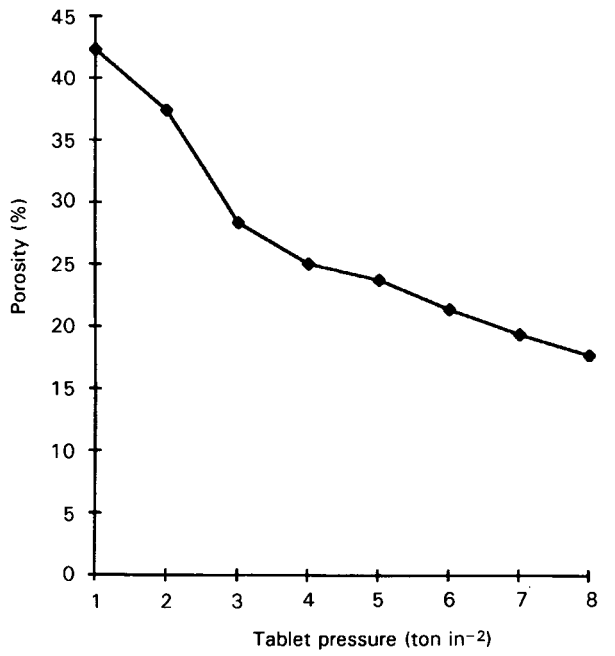

FIG. 11. Experimental and identical simulated porosity values for the eight tablets.

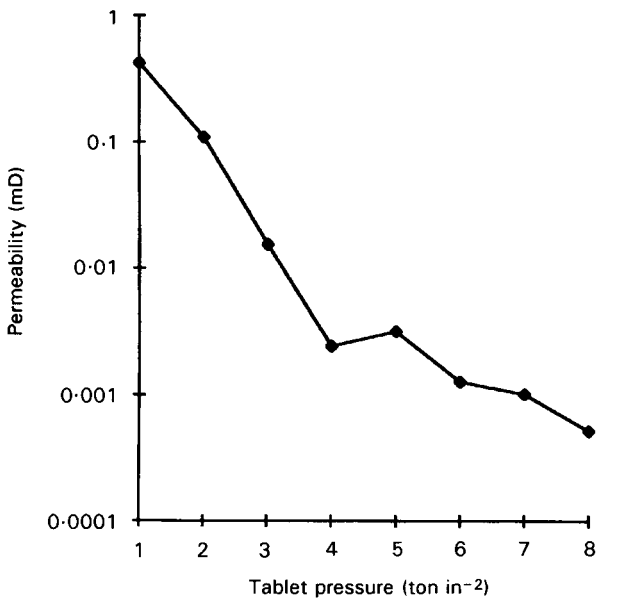

FIG. 10. Permeability values for the eight tablets.

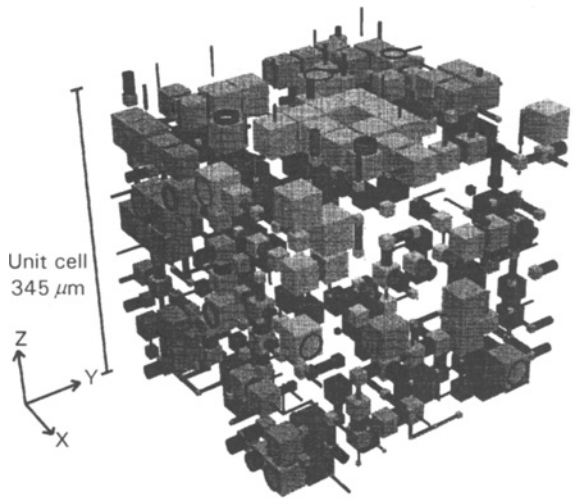

FIG. 12. Two outermost layers of the unit-cell for the 8-ton-in^{-2} tablet.

openness and large-pore voidage of the structure, reduces from 1·6 to 1·2 on compaction.

Conclusions

Eight tablets were pressed from a mixture of pharmaceutical grade crystalline lactose and an anti-inflammatory compound. The compacts were prepared at eight pressures over the range 1–8 ton in^{-2}. The experimental mercury-intrusion curves were measured and the data corrected using a spreadsheet-based program known as Pore-Comp. The corrected data were then used with Pore-Cor, the simulated mercury-intrusion curves being optimized to fit the experimental curves. The reduction in voidage in each sample as the pressure is increased is shown in the three-dimensional unit-cells produced by the simulation. Other properties have been investigated and related to the effects of the increasing pressure on the compacts. The changes in connectivity, throat-skew, pore-skew, experimental and simulated characteristic throat diameters, and simulated permeability and porosity are shown graphically. These parameters are difficult or impossible to measure experimentally. The successful void-structure modelling opens the way to improved understanding of important properties of compacts, chiefly strength, which depend on their void structure.

Acknowledgements

We thank the EPSRC for their financial support of this work.

References

Conner, W., Blanco, C., Coyne, K., Neil, J., Mendioroz, S., Pajares, J. (1988) Measurement of the Morphology of High Surface-area Solids: Inferring Pore Shape Characteristics. Characterization of Porous Solids, Elsevier, Amsterdam, pp 273–281

Gane, P., Kettle, J., Matthews, G., Ridgway, C. (1996) Void space structure of compressible polymer spheres and consolidated calcium carbonate paper-coating formulations. Ind. Eng. Chem. Res. 35: 1753–1764

Garboczi, E. (1991) Mercury porosimetry and effective networks for permeability calculations in porous materials. Powder Technol. 67: 121–125

Haines, W. (1927) Studies in the physical properties of soils. IV. A further contribution to the theory of capillary phenomena in soil. J. Agric. Sci. 17: 264–290

Koplik, J., Lin, C., Vermette, M. (1984) Conductivity and permeability from microgeometry. J. Appl. Phys. 56: 3127–3131

Leitritz, M., Krumme, M., Schmidt, P. C. (1996) Force–time curves of a rotary tablet press. Interpretation of the compressibility of a modified starch containing various amounts of moisture. J. Pharm. Pharmacol. 48: 456–462

Lu, G. Q., Shi, X. (1994) Computer simulation of isostatic powder compaction by random packing of monosized particles. J. Mater. Sci. Lett. 13: 1709–1711

Lustig, C., Adolfsson, A., Nyström, C. (1996) Studies on the surface-specific tensile strength of tablets. Eur. J. Pharm. Sci. 4 (Suppl.): S66

Mason, G., Mellor, D. (1991) Analysis of the Percolation Properties of a Real Porous Material. Characterization of Porous Solids II, Elsevier, Amsterdam, pp 41–50

Mason, G., Morrow, N. R., Walsh, T. (1988) Capillary Properties of Pores Formed by Two Unequal Parallel Rods and a Plate. Characterization of Porous Solids, Elsevier, Amsterdam, pp 243–154

Matthews, G., Spearing, M. (1992) Measurement and modelling of diffusion, porosity and other pore-level characteristics of sandstones. Mar. Pet. Geol. 9: 146–154

Matthews, G., Moss, A., Ridgway, C. (1995a) The effects of correlated networks on mercury intrusion simulations and permeabilities of sandstone and other porous media. Powder Technol. 83: 61–77

Matthews, G., Ridgway, C., Spearing, M. (1995b) Void space modelling of mercury intrusion hysteresis in sandstone, paper coating and other porous media. J. Colloid Interface Sci. 171: 8–27

Matthews, G., Ridgway, C., Small, J. S. (1996) Modelling of simulated clay precipitation within reservoir sandstones. Mar. Pet. Geol. 13: 581–589

Van Brakel, J., Modry, S., Svata, M. (1981) Mercury porosimetry: state of the art. Powder Technol. 29: 1–12

Wardlaw, N., Li, Y., Forbes, D. (1987) Pore-throat size correlation from capillary pressure curves. Transp. Porous Media 2: 597–614

Yanuka, M., Dullien, F., Elrick, D. (1986) Percolation processes and porous media I. Geometrical and topological model of porous media using a three-dimensional joint pore size distribution. J. Colloid Interface Sci. 112: 24–41